Continental Shelf Research 31 (2011) 73–84

Contents lists available at ScienceDirect

Continental Shelf Research

journal homepage: www.elsevier.com/locate/csr

Thermocline characterisation in the Cariaco basin: A modelling study of the thermocline annual variation and its relation with winds and chlorophyll-a concentration

A. Alvera-Azcárate [a,b,*], A. Barth [a,b], R.H. Weisberg [c], J.J. Castañeda [d], L. Vandenbulcke [a], J.-M. Beckers [a]

[a] AGO-GHER-MARE, University of Liège, Allée du 6 Août 17, B5, Sart Tilman, 4000 Liège, Belgium
[b] National Fund for Scientific Research, FNRS-FRS, Belgium
[c] University of South Florida, College of Marine Science, 140 7th Avenue South, 33701 Saint Petersburg, Florida, USA
[d] Instituto Oceanográfico de Venezuela, Universidad de Oriente, Camana-Sucre 6101, Venezuela

ARTICLE INFO

Article history:
Received 28 January 2010
Received in revised form
15 November 2010
Accepted 17 November 2010
Available online 24 November 2010

Keywords:
Thermocline depth
Hydrodynamic model
Model validation
Upwelling
Cariaco basin

ABSTRACT

The spatial and temporal evolution of the thermocline depth and width of the Cariaco basin (Venezuela) is analysed by means of a three-dimensional hydrodynamic model. The thermocline depth and width are determined through the fitting of model temperature profiles to a sigmoid function. The use of whole profiles for the fitting allows for a robust estimation of the thermocline characteristics, mainly width and depth. The fitting method is compared to the maximum gradient approach, and it is shown that, under some circumstances, the method presented in this work leads to a better characterisation of the thermocline. After assessing, through comparison with independent in situ data, the model capabilities to reproduce the Cariaco basin thermocline, the seasonal variability of this variable is analysed, and the relationship between the annual cycle of the thermocline depth, the wind field and the distribution of chlorophyll-a concentration in the basin is studied. The interior of the basin reacts to easterly winds intensification with a rising of the thermocline, resulting in a coastal upwelling response, with the consequent increase in chlorophyll-a concentration. Outside the Cariaco basin, where an open ocean, oligothrophic regime predominates, wind intensification increases mixing of the surface layers and induces therefore a deepening of the thermocline. The seasonal cycle of the thermocline variability in the Cariaco basin is therefore related to changes in the wind field. At shorter time scales (i.e. days), it is shown that other processes, such as the influence of the meandering Caribbean current, can also influence the thermocline variability. The model thermocline depth is shown to be in good agreement with the two main ventilation events that took place in the basin during the period of the simulation.

1. Introduction

The depth of the thermocline is crucial when modelling the physics of the ocean, as it largely affects the heat transfer between the ocean and the atmosphere, as well as the heat transfer between the ocean surface and deeper layers (Gill, 1982; Alexander et al., 2000). The thermocline positioning also affects the biological characteristics of the ocean such as the primary production (e.g. Muller-Karger et al., 1989; Di Lorenzo et al., 2005); it often determines the depth range at which nutrients are found, and the presence or not of phytoplankton, by establishing the separation between the warmer surface layer from deeper, cooler and nutrient-rich waters below the thermocline (Valiela, 1995). A correct characterisation of the thermocline is necessary for an accurate modellisation of the upper ocean dynamics and, in the case of coupled models, for a proper characterisation of the biomass and its location in the water column (Soetaert et al., 2001).

Upwelling-favorable winds over the coastal ocean result in a rising of isotherms, bringing the subsurface nutrient-rich waters to the surface, and inducing an increase of primary production in the surface layers, and hence of chlorophyll-a concentration. Situated in the Caribbean Sea, the Cariaco basin is affected by Trade winds and an upwelling is observed from November to May each year (Muller-Karger et al., 1989; Astor et al., 2003). In addition, rising isotherms outside of the basin might bring subsurface oxygenated water from the Caribbean Sea into the anoxic basin, because of its characteristic topography (Astor et al., 2003). A combination of in situ data, remote-sensing data and a numerical hydrodynamic model is used in this work to study the thermocline depth evolution inside and outside the Cariaco basin, and the relation of this variable with winds and chlorophyll-a concentration. The aim is to better understand how these variables are related and how the Cariaco basin is affected by the thermocline depth variability.

* Corresponding author at: AGO-GHER-MARE, University of Liège, Allée du 6 Août 17, B5, Sart Tilman, 4000 Liège, Belgium.
E-mail address: a.alvera@ulg.ac.be (A. Alvera-Azcárate).
URL: http://modb.oce.ulg.ac.be (A. Alvera-Azcárate).

0278-4343/$ - see front matter © 2010 Elsevier Ltd. All rights reserved.
doi:10.1016/j.csr.2010.11.006

A reliable method to calculate the thermocline depth in both the in situ data and the hydrodynamic model is needed. In addition, the accuracy of the hydrodynamic model in the representation of the thermocline depth needs to be assessed.

There are a number of works dealing with the calculation of the mixed layer depth. The mixed layer lies above the oceanic thermocline layer, and it is uniformly mixed due to the action of winds and solar heating. For example, Kara et al. (2000) use a threshold method in which a given increment in the temperature or density profile is identified as the position of the bottom of the mixed layer. Thomson and Fine (2003) use a split-and-merge method that approximates a specified curve using piecewise polynomial functions to find breakpoints that indicate the location of the mixed layer depth. Soetaert et al. (2001) use a fitting to a two-layer model to find the mixed layer depth in density and nitrate profiles.

On the other hand, this work describes a new technique to calculate the depth of the thermocline. Some works have previously dealt with this problem. For example, Palacios et al. (2004) and Kim and Miller (2007) use the maximum vertical temperature gradient to identify the depth of the thermocline. In this work we propose an alternative method to extract the depth and width of the thermocline from observed and modelled temperature profiles. Our approach consists in fitting individual temperature profiles to sigmoid curves, in a least-square approach. This method is similar to the one used by Steyn et al. (1999) to determine the height of the atmospheric entrainment zone (a concept equivalent to the thermocline in the ocean), and it provides not only the depth of the thermocline but also the width of this layer. The width of the thermocline layer gives information on the steepness of the temperature gradient, which in turn indicates the availability of tracers like nutrients from the subsurface layers.

Once the thermocline depth and width are known, the error between model and observations can be then analysed separately for various components: the error in the positioning of the thermocline, the error of the temperature at the thermocline depth and finally an error of the thermocline layer width. These three error measures provide information on the amount of mixing induced by the model and the transfer of heat through the surface and subsurface water layers. This information can be a useful feedback for model calibration processes: an error in the depth of the thermocline directly affects the heat transfer in the upper layers of the ocean and the atmosphere; an error in the thermocline width will have an impact in the heat transfer among surface and deeper layers, and can also affect species concentration and vertical migration in coupled biological models; finally, an error in the temperature of the thermocline might as well indicate that the heat transfer from the surface is too high, or that an overall bias is present in the model.

This work is organised as follows: the domain of study, data and numerical model used on this work are described in Section 2. Section 3 introduces the fitting method for temperature profiles and compares its accuracy with the maximum-gradient method. The model thermocline error analysis is shown in Section 4. A study of the annual variation of the thermocline depth in the Cariaco basin and its relation to wind intensity and chlorophyll-a concentration is presented in Section 5, along with a study of the ventilation events observed in the basin. The conclusions of this paper are presented in Section 6.

2. Materials

2.1. Study area

The Cariaco basin is a semi-enclosed area off the coast of Venezuela. Two shallow passages (the Centinela channel to the west and the Tortuga channel to the northeast) connect the upper 150 m of the basin to the open ocean. The basin interior, with a maximum depth of 1400 m, is therefore completely isolated from the open ocean, and the ventilation of the basin waters is done only through the upper layers. Waters deeper than 250 m are anoxic in the Cariaco basin, with very limited changes in temperature, salinity and other properties (Astor et al., 2003). A detailed description of the basin hydrography can be found in, e.g. Muller-Karger et al. (2001), Astor et al. (2003), Alvera-Azcárate et al. (2009a), Muller-Karger et al. (2010). Accurate modelling of the surface waters that connect the Cariaco basin with the open ocean is very important in order to correctly simulate the temperature, salinity and currents in the basin's interior. Moreover, a correct characterisation of the thermocline width and depth will determine if the ventilation of the basin is accurately represented by a model (i.e. if water of Caribbean origin is able to enter into the Cariaco basin). The results from a hydrodynamic model of the Cariaco basin described in Alvera-Azcárate et al. (2009a) are analysed in this work.

2.2. In situ and satellite data

A series of 35 CTD casts were taken between 15 and 19 March 2004 in the eastern part of the Cariaco basin (Fig. 1), in the framework of the carbon retention in a colored ocean (CARIACO) time series program (Muller-Karger et al., 2010). These CTD profiles are used in this work to asses the ability of a hydrodynamic model of the Cariaco basin (Alvera-Azcárate et al., 2009a) to reproduce the thermocline depth and width. The hydrodynamic model was validated in Alvera-Azcárate et al. (2009a), but no analysis of the thermocline depth was done. The CTD data available for this work are averages over 19 depth levels, with a refinement in the surface layer (11 out of the 19 depth levels are concentrated at the top 200 m of the water column). Data from monthly cruises made during 2004 at the CARIACO station ([10.5°N; 64.68°W], see location in Fig. 1) are also used. In particular, temperature and continuous dissolved oxygen profiles are used. Details on the processing of these data can be found in Astor et al. (2003). All in situ data were realised aboard the R/V Hermano Ginés, from the Fundación La Salle de Ciencias Naturales of Venezuela, and have been accessed through the project website, http://www.imars.usf.edu/CAR/.

Satellite chlorophyll-a concentration data are also used in this work. The data are obtained from the sea-viewing wide field-of-view sensor (SeaWiFS), on board the SeaStar spacecraft (http://oceancolor.gsfc.nasa.gov/), with a spatial resolution of about 11 km in the study zone. The data are 8-day composites and contain a small percentage of clouds (about 22%) that have been removed using DINEOF (data interpolating empirical orthogonal functions), an EOF-based technique to reconstruct missing data (Beckers and

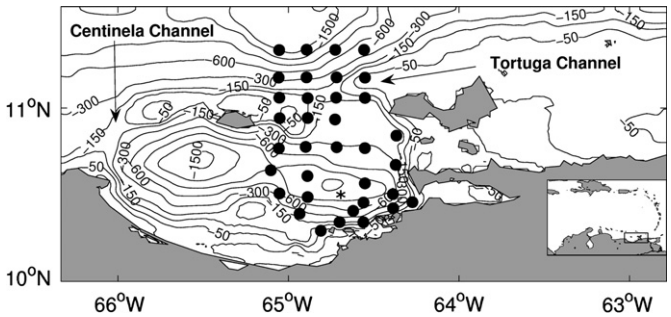

Fig. 1. The Cariaco basin. Contours show the bathymetry, and the circles show the position of the 35 CTD profiles measured in March 2004. The asterisk shows the location of the CARIACO station. The small insert map shows the location of the Cariaco basin in the Caribbean Sea.

Rixen, 2003; Alvera-Azcárate et al., 2005, 2007). DINEOF uses the mean and covariance of the original data to calculate an EOF basis, which in turn it is used to calculate the missing data. If the original data are normally distributed, then the probability density distribution can be completely described by their mean and the eigenvectors of the covariance matrix (the EOFs). Variables such as chlorophyll-a concentration, however, do not have a Gaussian distribution, since this variable is never smaller than zero. This is not taken into account in the EOF decomposition. To overcome this, a logarithmic transformation of the chlorophyll-a data has been performed before using DINEOF. An exponential function has been taken afterwards to retrieve the initial units. A total of seven EOFs have been used for the DINEOF reconstruction, a number determined by cross-validation. The error of the reconstruction is 1.5 mg m^{-3}.

2.3. Hydrodynamic model

A simulation of the Cariaco basin hydrodynamics for the year 2004 (Alvera-Azcárate et al., 2009a) is used in this work. The model is based on ROMS (Shchepetkin and McWilliams, 2005), and it is nested in the $1/12^{\circ}$ global navy coupled ocean data assimilation (NCODA) HYCOM (hybrid coordinate ocean model, Chassignet et al., 2007). The Cariaco model is a three-dimensional, free-surface and hydrostatic primitive equations model. It has 32 vertical terrain-following levels, and a horizontal resolution of $1/60^{\circ}$, i.e. 1.82 km × 1.85 km in the zonal and meridional directions, respectively. Mellor and Yamada (1982) used 2.5 turbulence closure scheme. Open boundary conditions for temperature, salinity, elevation and currents are obtained daily from HYCOM. The atmospheric forcings are provided by National Centers for Environmental Prediction (NCEP, Kalnay et al., 1996) for the thermodynamic forcing (air temperature, relative humidity, cloud fraction and short wave radiation), winds and surface net freshwater flux (evaporation–precipitation flux), while long wave radiation, latent and sensible heat are calculated interactively by the model using bulk formulae (Fairall et al., 1996). Sea surface temperature (SST) is corrected by relaxing to a cloud-free advanced very high resolution radiometer (AVHRR) SST field (http://podaac.jpl.nasa.gov/poet), calculated following Alvera-Azcárate et al. (2005). More information on this model implementation and validation can be found in Alvera-Azcárate et al. (2009a), and the nesting procedure is further explained in Barth (2008a,b).

3. Method

3.1. Characterisation of thermocline by a least-squares fit to a sigmoid function

In order to find the position and width of the thermocline, each temperature profile is adjusted to a sigmoid curve, in the least-squares sense. A sigmoid function can be defined by

$$s(z) = T_u + \frac{T_b - T_u}{1 + e^{((z-D)/2W)}} \quad (1)$$

where z is the depth profile, T_u and T_b are the temperature at the top and bottom of the thermocline respectively, D is the depth of the middle of the thermocline and W is the width of the thermocline. The optimal values of these four parameters (shown in Fig. 2) are calculated through the fitting, to adjust each temperature profile to a sigmoid function by minimising the residuals between the two curves. Additional constraints are given (Coleman and Li, 1996) as the maximum and minimum possible values for each of these parameters, in order to force the fitting not to reach unrealistic values (as, for example, a thermocline depth above the water). The temperature of the profile at the thermocline depth ($z=D$) is obtained by interpolating the temperature to the depth calculated by the fit.

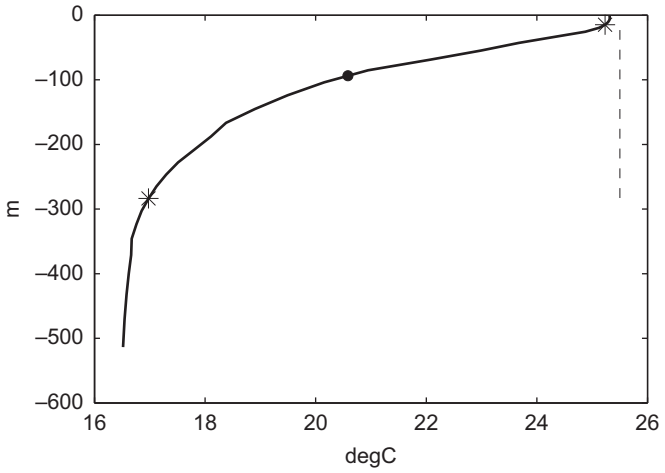

Fig. 2. Parameters obtained through the sigmoid fitting of a temperature profile. Asterisks show the upper and lower limits of the thermocline layer, the circle shows the central position of the thermocline, and the dashed line shows the width of this layer.

The residuals of the least-squares adjustment ($r=y(z)-s(z)$, with $y(z)$ the original temperature profile) give an idea of the overall mismatch between the sigmoid curve and the temperature profile. A large residual means that the temperature profile itself does not follow a sigmoid trajectory. However, the fitting method still situates the largest gradient of the sigmoid curve in the region of largest temperature change, so that the thermocline depth is successfully detected even when non-sigmoid temperature profiles are used. This is shown in Fig. 3 for three examples: one at the Tortuga channel, one inside the basin and one outside the basin. When the temperature profile presents a clear sigmoid form (as for the profiles at the Tortuga channel and inside the basin), small residuals between the temperature profile and the fitted profile are obtained. The largest residuals are found outside the Cariaco basin, where the temperature profile presents a decreasing exponential form, rather than a sigmoid form. The detection of the thermocline depth is however correct in the three cases, as the zone of largest temperature change is correctly detected by the fitting method in all profiles.

The fitting method is applied to temperature profiles in this work, although it can also be applied to other variables, as for example, density profiles. In that case, the pycnocline depth would be obtained, along with the density at the top and bottom of this layer, and its width. All these parameters are linked to the internal radius of deformation, an important spatial length in the ocean.

3.2. Comparison with maximum-gradient method

An alternative way to calculate the thermocline depth is to directly find the depth where the vertical gradient of temperature reaches its maximum ($\delta T/\delta z$), a technique employed by Palacios et al. (2004) and Kim and Miller (2007). $\delta T/\delta z$ is calculated for each depth level, starting from the surface. Although the maximum gradient is generally an accurate technique, several limitations become evident when applying it to the temperature profiles: the presence of noise or features like a diurnal thermocline might lead to inconsistent results, and the fact that the maximum gradient is limited in the calculation of the thermocline depth to the discrete

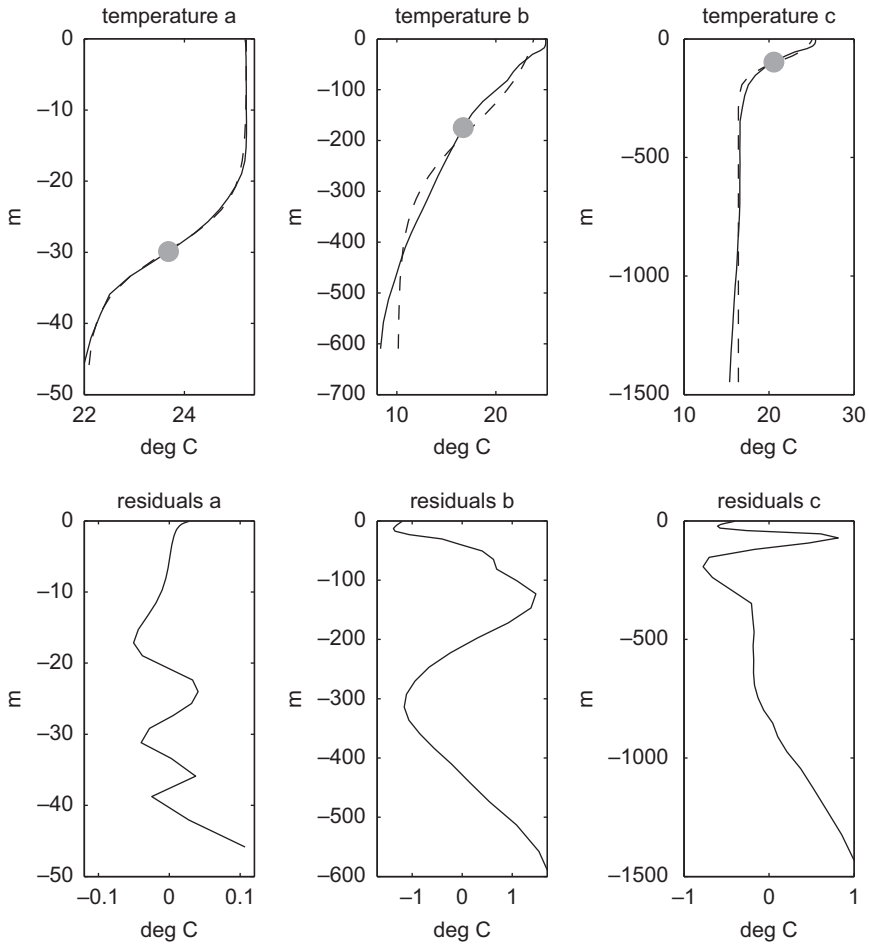

Fig. 3. Top panel: examples of temperature profiles (solid line) and fit (dashed line), along with the thermocline depth detected by the fitting technique. Bottom panel: corresponding residuals of the fit (sigmoid curve minus temperature profile). Large residuals indicate the deviation of the profile from the sigmoid curve, although even when residuals are large, the thermocline depth is accurately detected. The date of the profiles shown is 15 March 2004 and the three locations are: (a) the Tortuga channel [10.9°N; 65°W]; (b) outside the Cariaco basin [11.3°N; 65.35°W]; (c) inside the Cariaco basin [10.7°N; 65.5°W]. Note that the depth and temperature ranges are different for each location.

depths of the initial temperature profile. For example, in the temperature profiles used in this work there is a measurement at 35 m, and the following one is at 55 m depth, which means that if the thermocline is at 45 m depth, the thermocline depth will be detected with an error of 10 m. The sigmoid fit method is not limited to the initial depth levels of the profile, therefore avoiding such errors.

Fig. 4 shows four profiles, along with the thermocline depth detected by the maximum gradient method and the sigmoid fit method. The two first panels show examples in which both methods agree in the depth of the thermocline. However, due to the discrete depths of the initial profiles, the thermocline depth detected for the second profile is too shallow for the maximum gradient approach. The two lower panels show examples in which both methods disagree, with the result given by the sigmoid fit method being clearly more accurate. For example, in the fourth panel the maximum gradient is situated at the diurnal thermocline instead than at the permanent thermocline. A small change in the temperature profile can lead therefore to very different results with the maximum gradient method. The fitting method in the present work leads to more robust results, as it detects the permanent thermocline in the two lower panels. It is therefore expected that the fitting technique is less sensitive to the presence of noise or errors in the temperature profiles.

4. Error analysis of the Cariaco model thermocline

The depth and width of the thermocline have been calculated for the two CTD data sets mentioned in Section 2 (CTDs taken from 15 to 19 March and the monthly CTDs taken at the CARIACO station) using the fitting technique. The model results have been interpolated to the observation locations, and the fitting technique has been applied to these profiles. The temperature at the center of the thermocline layer has also been calculated for all data sets. The model thermocline depth and width can be then compared to the observations. Table 1 presents a summary of the model thermocline error. Also given are the corresponding standard deviations. The average observed thermocline depth is -66.7 m and -78.4 m for the model. Regarding the average width of the thermocline, it is 51.9 m for the observed profiles and 61.9 m for the modelled profiles.

The model presents a negative bias in the depth of the thermocline, i.e. the thermocline is too deep compared to observations (Table 1). The average RMS error in the positioning of the thermocline model is 31.58 m, which is smaller than the standard deviation of both observations and model. The model thermocline is too wide (positive bias of 9.99 m), with an RMS error of 33.64 m. The model thermocline is thus wider and deeper than observed, which might be indicative of an excessive mixing of the surface

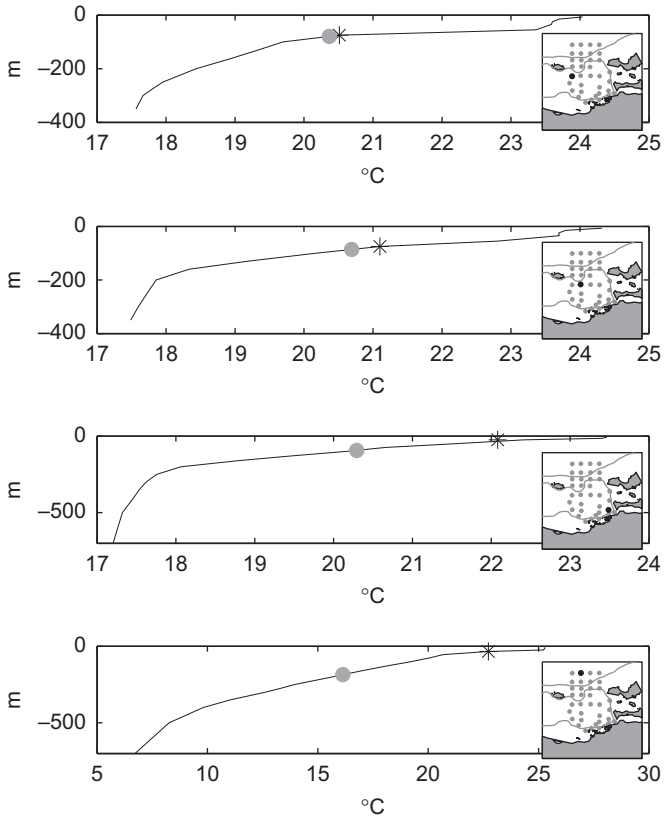

Fig. 4. Comparison of the fitting method with the maximum gradient method for four temperature profiles (see position in the small map inserts). The asterisk represents the depth of the thermocline as detected by the maximum gradient method, and the gray circle represents the thermocline depth as calculated by the sigmoid fit method presented in this work.

Table 1
Bias, root mean square error (RMS) and correlation (r) of the model thermocline with respect to the 35 CTDs taken during March 2004. The errors are decomposed in depth, temperature and width. All correlation coefficients are significant at the 99.99% level. Lower rows: standard deviation (σ) of observations and model for the depth, temperature and width of the thermocline.

	Depth	Temperature	Width
Bias	−11.71 m	−0.6 °C	9.99 m
RMS	31.58 m	1.29 °C	33.64 m
r	0.79	0.8	0.77
σ_{obs}	39.25 m	1.81 °C	44.34 m
σ_{mod}	48.94 m	1.83 °C	49.65 m

layers. Regarding the temperature at the center of the thermocline layer, a small bias (−0.6 °C) and RMS error are found (see Table 1).

When the monthly CTDs taken at the CARIACO station were used, the model presents bias of −10 m in depth and of 2.32 m in width. RMS errors are of 17.0 and 34.78 m respectively. The model shows therefore a good agreement with this data set.

A comparison between four modelled and observed temperature profiles from the March campaign is shown in Fig. 5. The modelled profiles are able to represent the thermocline depth accurately at various locations inside and outside the Cariaco basin, compared to observations (see top and middle panels of Fig. 5). At shallower depths, as for the profiles located near the Tortuga channel (panels b and c of Fig. 5), the model differs the most from observations because of a cold bias (panel c) or because the model has a slightly shallower thermocline than observed. This region around the Tortuga channel was identified as the zone with the highest errors between observations and model, and the cause was attributed to the higher variability of an exchange channel (Alvera-Azcárate et al., 2009a). Inside and outside the Cariaco basin (panels a and d of Fig. 5) the model represents accurately both the vertical distribution of temperature and the depth of the thermocline. A simple RMS difference between the observed and the modelled profiles would not reveal which aspects of the thermocline are accurately represented or not, an analysis that can be easily done with the technique presented in this work.

5. Description of the thermocline in the Cariaco basin

The results presented so far indicate that the technique used to calculate the thermocline depth gives accurate and robust results, and that the model compares reasonably well with available observations for a variety of profile forms. Given these results we will analyse the annual cycle of the model thermocline depth in the Cariaco basin, and how it relates to variables such as wind and chlorophyll-a concentration. The depth of the thermocline at the channels that communicate the Cariaco basin with the open ocean is a crucial parameter in the ventilation of the interior of the basin. As an anoxic basin, an important oxygen source comes from the subsurface Caribbean Sea waters that enter through the Cariaco basin channels.

For every day during the simulation period and for every water column in the model domain, the characteristics of the thermocline have been computed, so two-dimensional fields of the thermocline depth and width are obtained for each day of the model simulation. These fields are used in this section to study the temporal and spatial evolution of the thermocline, and its relation with other variables, such as winds and chlorophyll-a concentration.

5.1. Spatial and temporal evolution of the thermocline

Fig. 6 shows the spatial average and standard deviation of the thermocline depth in the Cariaco model for 2004. Inside the Cariaco basin the average depth of the thermocline is about 100 m, and outside the basin, in deeper waters, the thermocline reaches an average of more than 200 m. Depth contours are included in the figure, showing that in general, the depth of the domain constrains the average depth of the thermocline. The standard deviation of the thermocline depth is also an indicator of the baroclinic variability of the ocean. The variability of the thermocline (bottom panel of Fig. 6) is also constrained by the bathymetry. The thermocline depth variability around the Tortuga channel is higher than inside the basin, which may be due to the exchanges with the open ocean that take place across this channel. The variability at the Centinela channel is smaller.

The average and standard deviation of the thermocline width (not shown) have a spatial distribution similar to the one presented in Fig. 6 for the thermocline depth. Inside the Cariaco basin, the average thermocline width is about 150 m, and outside the basin it reaches 400 m. The standard deviation is of 20–30 m inside the Cariaco basin, with the highest values in the eastern part, near the Tortuga channel. Outside the basin, the standard deviation reaches a maximum of 60 m.

In Fig. 7, the seasonal anomalies of the thermocline depth (with respect to the mean presented in Fig. 6) are shown. Positive/negative anomalies indicate a shallower/deeper thermocline than the mean field, respectively. The thermocline inside the Cariaco basin deepens through the year, while outside the basin a rising trend is observed. One might expect that the thermocline characteristics of the end of 2004 should be similar to those of the beginning of 2004, if the annual cycle is to be repeated in 2005.

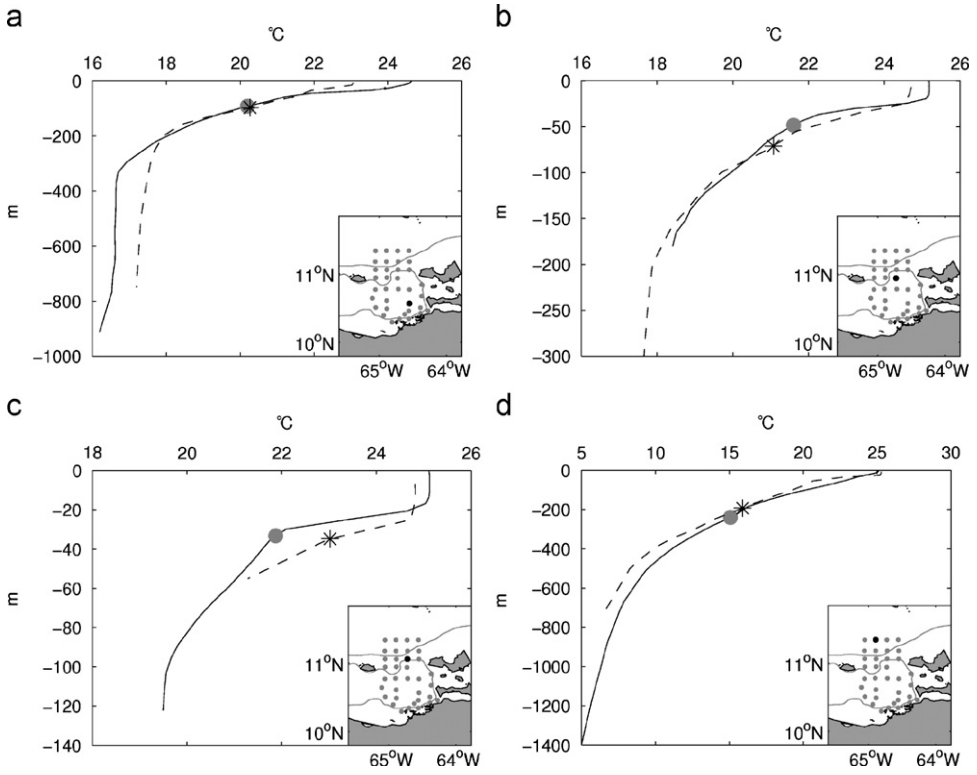

Fig. 5. Observed (dashed line) and modelled (solid line) profiles at four locations in the Cariaco basin domain (two inside the basin, one at the Tortuga channel, and one outside the basin). The asterisk and the grey circle show the thermocline depth for the observed and modelled profile respectively. Small insert maps show the position of the profiles with a black circle, and the 200 m isobath as a thin black line.

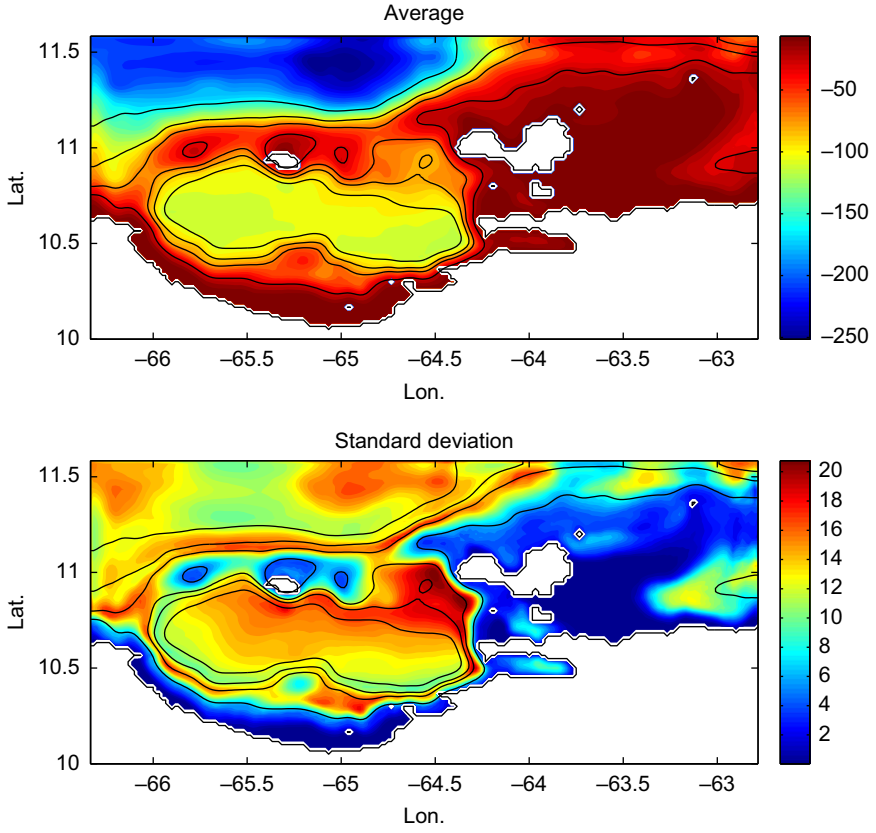

Fig. 6. 2004 spatial average (top) and standard deviation (bottom) of the thermocline depth (in m) of the Cariaco basin model. Black contours show the 50, 150, 250 and 500 m isobaths.

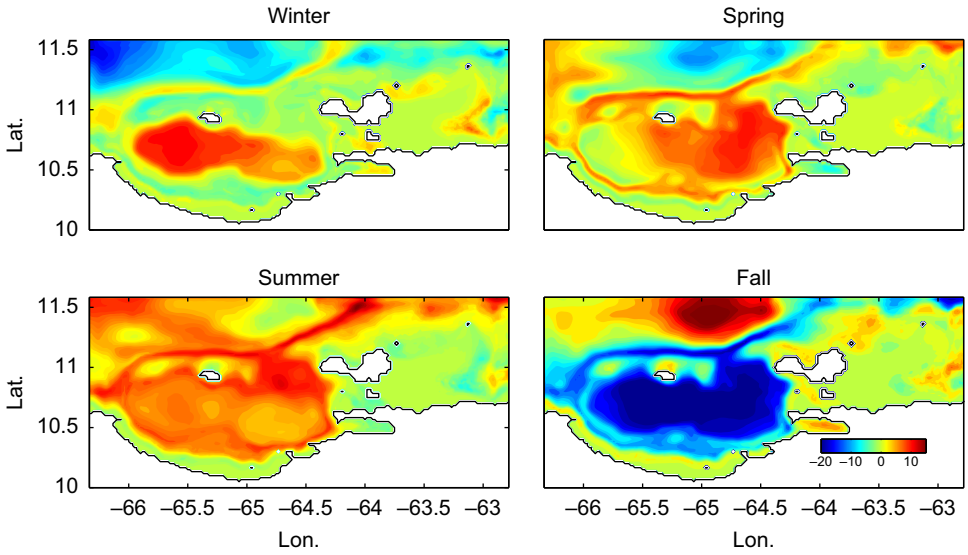

Fig. 7. Spatial average of the thermocline depth anomalies calculated for each season in the Cariaco model (winter: January–March; spring: April–June; summer: July–September; fall: October–December). The average field of Fig. 6 has been removed from each season.

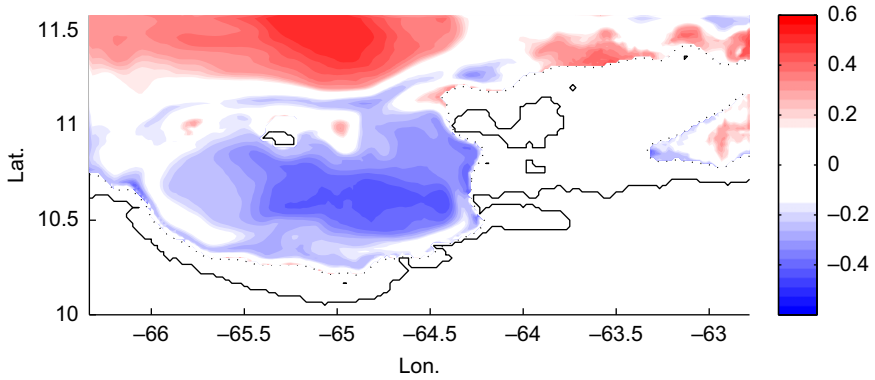

Fig. 8. Correlation between the easterly component of the wind and the depth of the thermocline layer. The black line shows the coastline and the dashed line shows the 30 m depth contour.

As this appears not to be the case, the variation of the advanced very high resolution radiometer (AVHRR) sea surface temperature over the domain was examined: the average surface temperature within the basin indeed increased about 2 °C from January 2004 to December 2004 (not shown), so 2004 ended warmer than it began. This can explain the difference in thermocline depth: as more heat is available for the air–sea exchanges, the thermocline deepens through the year, and it does not recover at the end of the year. This leaves the question open as to whether this year showed an anomalous deepening of the thermocline, or if the recovering of the thermocline to depths typical of winter takes place rapidly at the onset of the winter season. This should be addressed in the future with multi-year runs of the Cariaco basin model.

5.2. *Relationship between the thermocline depth, winds and chlorophyll-a concentration*

Strong north-easterly winds characterise the Caribbean Sea most of the year. These winds become weaker during summer months, when a southern component develops, therefore winds are mainly south-easterly during this part of the year (Muller-Karger et al., 2001). Dynamically, the thermocline is affected by the winds, and in this section we study how the winds used to force the model affect the width and depth of the thermocline in the Cariaco basin. An upwelling develops in the Cariaco basin as a response to the prevalent winds, therefore we will also compare the evolution of the thermocline to satellite chlorophyll-a concentration fields. These analyses are realised to better understand the dynamics of the Cariaco basin, and the relationship between these three variables. In addition, the study of the relationship between the thermocline depth and chlorophyll-a concentration will also serve as an indirect validation of the model results with an independent variable.

Figs. 8 and 9 show the correlation between the easterly component of the NCEP winds described in Section 2 and the depth and width of the thermocline in the model domain, respectively. Stronger easterly winds cause the thermocline to rise and become sharper (decreased width) inside the Cariaco basin, probably explained by the upwelling mechanism. An asymmetry is observed inside the basin, with the strongest correlation situated in the eastern part of the basin. Note the opposite behaviour of the thermocline inside and outside the Cariaco basin to the same wind forcing (the NCEP wind field used has little spatial variation over the whole domain): outside the basin, stronger easterlies increase the mixing of the surface layers, resulting in a deeper and wider

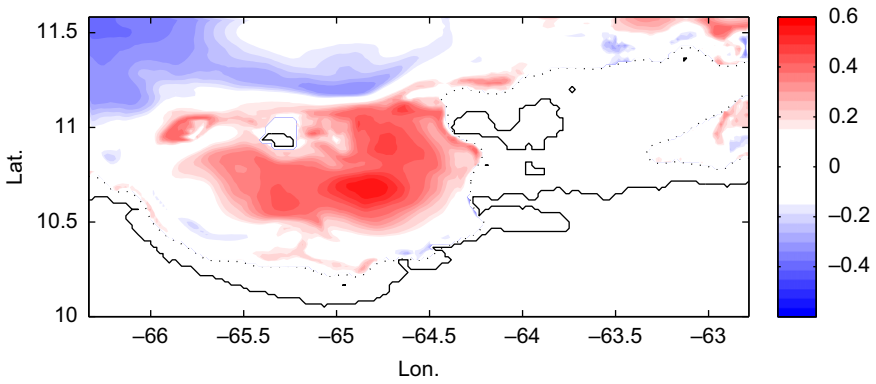

Fig. 9. Correlation between the easterly component of the wind and the width of the thermocline layer. The black line shows the coastline and the dashed line shows the 30 m depth contour.

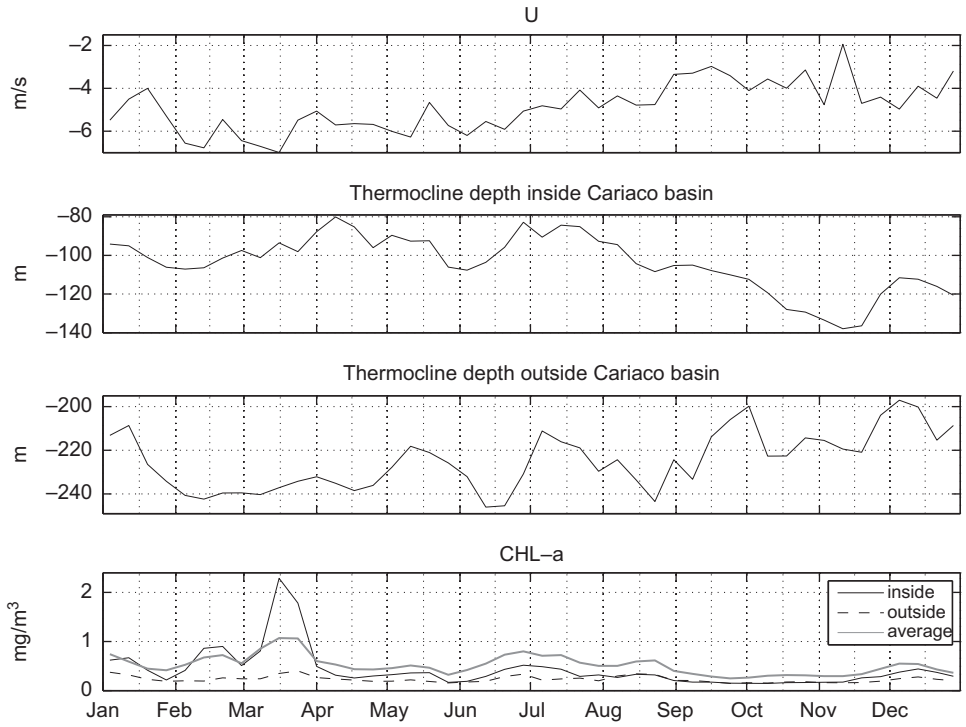

Fig. 10. From top to bottom: 2004 annual variation of the easterly component of the wind (average over the study domain presented in Fig. 1), depth of the thermocline inside and outside the Cariaco basin, and concentration of satellite-derived chlorophyll-a (inside the basin [10.5°N; 65°W to 11°N; 64.6°W] outside the basin [11°N; 66.3°W to 11.7°N; 65.4°W] and averaged over the study domain). Labels indicate the first day of each month.

thermocline in that zone when winds are stronger. Two distinct regimes can be therefore described in the Cariaco basin: an inshore domain affected by the topography, and an open ocean domain, mostly affected by large scale ocean and atmosphere dynamics. The correlation between the depth of the thermocline and the easterlies component of the wind is −0.48 inside the Cariaco basin, and 0.54 outside the Cariaco basin (significant at the 99% and 99.9% level respectively). There is no significant correlation between the thermocline depth and width and the north–south component of the wind.

Satellite chlorophyll-a concentration fields show that the highest concentrations occur at the eastern part of the basin (Muller-Karger et al., 1989), where the upwelling response is stronger. To compare with these data, the winds and the thermocline depth are averaged to the 8-day temporal resolution of the chlorophyll-a data set. A time series of the easterly component of the wind averaged over the domain is shown in Fig. 10, together with time series of the depth of the thermocline at two points of the studied domain (one inside the basin, at [64.7°W; 10.6°N] and another outside the basin, at [65.02°W; 11.3°N]). In addition, time series of chlorophyll-a concentration are also shown, one representing an average inside the basin, one representing an average outside the basin and finally the chlorophyll-a concentration averaged over the whole domain. As mentioned, easterly winds become weaker through the year, with higher winds in spring and the weakest winds at the end of summer. The stronger spring winds produce an upward displacement of the thermocline, steadily rising from 100 m depth to about 80 m depth from winter to spring 2004. The primary peak of chlorophyll-a concentration is observed at the end of March over the Cariaco basin domain, with a secondary peak in summer (lower panel of Fig. 10), as it has also been observed in satellite and in situ data during other years (e.g. Muller-Karger et al., 1989, 2001).

The evolution of the thermocline depth and chlorophyll-a concentration confirm that an upwelling mechanism initiates inside the basin, when nutrients are brought to the surface waters through the rising of the thermocline due to the action of wind. The correlation between chlorophyll-a concentration and thermocline depth inside the basin is 0.61 (significant at the 99.9% level).

Again, the situation outside the Cariaco basin is the opposite as in the interior: along with stronger winds, a deeper thermocline is observed. This means that the nutrients are located deeper in the water column, and therefore the concentration of chlorophyll-a in the surface layers is lower outside the Cariaco basin. The correlation between chlorophyll-a concentration and thermocline depth outside the Cariaco basin is −0.41 (significant at the 99% level). A summary of the correlation between the three variables is given in Table 2.

Table 2
Correlation between chlorophyll-a concentration (CHL-a), the easterly component of the wind (U) and the depth of the thermocline inside the Cariaco basin (Depth_i) and outside the Cariaco basin (Depth_o).

	CHL-a	U	Depth_i
U	−0.63		
Depth_i	0.61	−0.48	
Depth_o	−0.41	0.54	−0.32

5.3. Thermocline depth and ventilation of the basin

The rising of the thermocline outside the Tortuga and Centinela channels might bring oxygenated, Caribbean subsurface waters into the Cariaco basin, an event know as ventilation (e.g. Scranton et al., 2001; Astor et al., 2003). Given the anoxic environment from about 250 m to the bottom of the basin, these ventilation events can have a high impact in the physical, chemical and biological characteristics of the basin.

To determine whether the position of the thermocline can give us some information about when these ventilation events might happen, we have examined how the thermocline depth varies in a transect across the Tortuga channel. Fig. 11 shows the daily evolution of the thermocline along this transect (position shown in the small insert of the figure) during the year, along with the winds. The difference between the thermocline depth at the two edges of the transect is also included, which can be seen as the slope of the thermocline along the transect. The more negative its value, the higher the slope, with a deeper thermocline always outside the basin.

A relationship at long time scales (seasonal to semi-annual) between the strength of the easterly component of the winds and the thermocline slope along the transect is seen (with a correlation of −0.4, significant at the 99.9% level): stronger winds cause a steeper slope across the channel, and when winds relax, the difference in thermocline depth inside and outside the basin decreases. It could then be expected a higher possibility for a

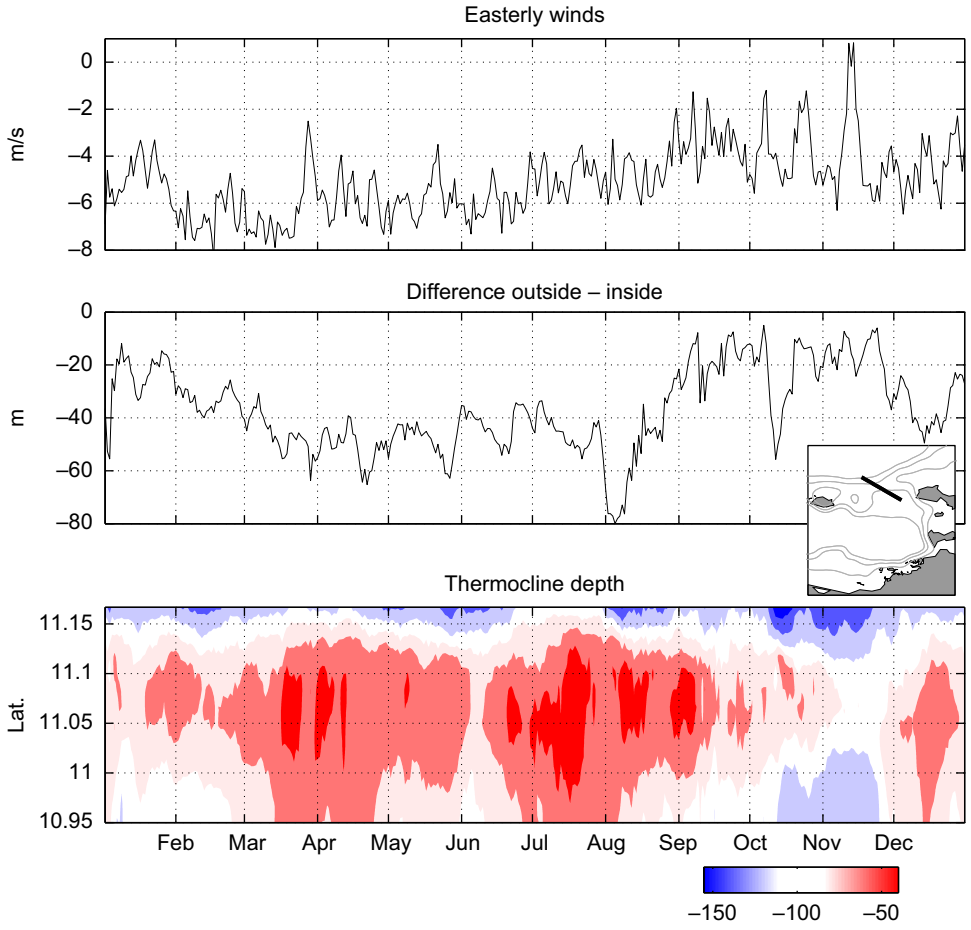

Fig. 11. Upper panel: easterly winds over Cariaco basin domain. Middle panel: difference between the thermocline depth at the edges of the transect (proxy for thermocline slope) shown in the small insert map. Bottom panel: thermocline depth (m) along the transect.

ventilation event when winds are weak, i.e. from September to November. However, as it can be observed in the bottom panel of Fig. 11, the decrease in slope observed from September to November is mainly due to a deepening of the thermocline inside the basin, and not because of a rising of the thermocline outside the basin. It is therefore important to observe the evolution of the thermocline depth across the Tortuga channel to gain insight on the ventilation events on the Cariaco basin.

At shorter time scales, the relationship between winds and thermocline depth is not so evident. There are however instances with a good correspondence between high-wind events and the response in the thermocline depth (e.g. in mid-October a sudden increase in wind intensity, from -2 to $-4\,\mathrm{ms}^{-1}$ in two days, causes an increase in the thermocline slope). However, other short-term changes in the thermocline slope across the Tortuga channel do not correspond to changes in the wind field. For example, at the beginning of August there is a high increase of the thermocline slope across the Tortuga channel, but no strong change is observed in the wind intensity. This event was documented in Alvera-Azcárate et al. (2009a): the passage of a cyclonic eddy on the Caribbean Current originated an outflow of Cariaco waters into the Caribbean Sea. It can be seen in Fig. 11 that the thermocline depth also responded to the influence of the eddy, deepening outside the Tortuga channel and rising inside the Cariaco basin. A similar behaviour was described in Astor et al. (2003) for the period 1996–1998. This example highlights that, although long-term variability of the ocean thermocline depth responds to atmospheric conditions, at shorter time-scales other processes play an important role.

Looking at the evolution of the thermocline across the Tortuga channel, at some instances (from mid-March to mid-April and during July) the thermocline rises both inside and outside of the Tortuga channel (Fig. 11, bottom panel), reaching about 100 m outside the basin and about 50 m inside the basin. The thermocline is then well above the sill depth, and therefore the entrance of Caribbean subsurface waters into the Cariaco basin is possible during those periods.

To verify if the thermocline depth across Tortuga channel is helpful in identifying ventilation events, we calculated the depth of the oxic–anoxic interface as described in Astor et al. (2003). Using the oxygen monthly profiles described in Section 2, we calculated the depth of the oxic–anoxic interface as the depth at which the concentration of oxygen is not detectable by the sensor (i.e. concentrations $\leq 5\,\mu\mathrm{M}$, following Astor et al., 2003). The results are shown in Fig. 12, in which we see that maximum oxic–anoxic interface depths were reached in April, June–July and October–November. One should note that none of the ventilation events registered in 2004 were as intense as those shown for the period 1996–1998 in Astor et al. (2003), when maximum depths of 320 m were reached. In addition, the oxygen profiles are measured in the middle of the Cariaco eastern sub-basin, so it is possible that some ventilation events are missed by these measurements, if water enters from the Centinela channel, or if it sinks directly from the Tortuga channel to depths higher than 300 m (and therefore no migration of the oxic–anoxic interface is recorded at the measuring location). Given these limitations, we can conclude there is a good agreement between the model thermocline depth at the Tortuga channel and the ventilation events. The September–November event suggested by the thermocline slope across Tortuga channel is less evident in the oxygen data.

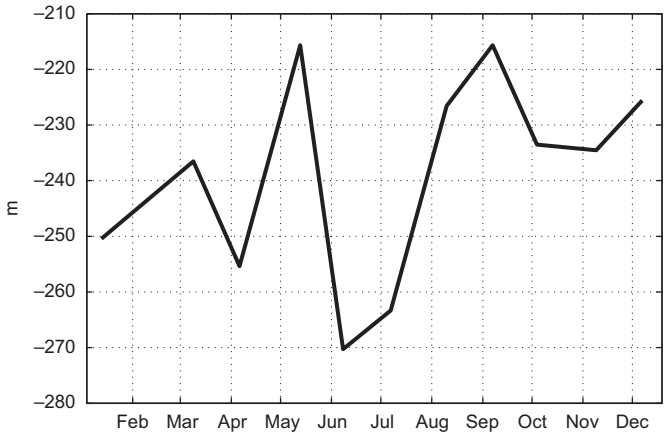

Fig. 12. Estimation of the monthly oxic–anoxic interface depth at the CARIACO station during 2004.

It has been shown in previous studies (Astor et al., 2003; Alvera-Azcárate et al., 2009a) that the rising of isotherms at the Tortuga channel coincides with the passage of an anticyclonic eddy along the Caribbean Current. We have verified the presence of such eddies in sea surface height data for both ventilation events. Sea surface height data were provided by Collecte, Localisation, Satellites (CLS), Le Traon et al. (1998) and Ducet et al. (2000), and the description of the data set and processing are detailed in Alvera-Azcárate et al. (2009b). However, anticyclonic eddies were also present at other moments of the year (there is an average of 4.3 eddies per year traveling along the Caribbean Current, Alvera-Azcárate et al., 2009b). Therefore, although the ventilation of the Cariaco basin appears to occur when an anticyclonic eddy approaches the basin, not all anticyclonic eddies traveling along the Caribbean Current results in the ventilation of the basin. The positioning and strength of these eddies are important factors, as well as the particular state of the Cariaco basin when the eddies approach the basin, such as the dominant currents or the vertical structure of the water column.

6. Conclusions

A technique has been described to calculate the depth and width of the thermocline, based on a fitting of temperature profiles to a sigmoid curve. The method described is able to accurately characterise the thermocline for different profile forms. It has been shown to give more robust results than the maximum gradient technique in cases when, for example, a secondary (diurnal) thermocline is present. The method has been applied to the Cariaco basin temperature profiles from a hydrodynamic model, in order to assess the capability of the model to represent the Cariaco basin thermocline.

The model thermocline depth and width have been compared to a series of CTD casts taken during March 2004 in the Cariaco basin, as well as to a series of monthly CTDs taken at the CARIACO station. This analysis has shown that the model mixing is probably too high in the model, since the thermocline appears to be too deep and too wide compared to in situ observations. It would be suggested, as future work, to study different mixing schemes and to assess which scheme provides the most realistic thermocline depth in the basin. This application shows that the characterisation of the thermocline depth and width helps to better understand the nature of the model errors.

A significant correlation was detected between the model thermocline depth inside the Cariaco basin and the concentration of chlorophyll-a, with shallower thermocline depths corresponding to a higher chlorophyll-a concentration. This relationship is the opposite outside the basin. The chlorophyll-a concentration is an independent data set with regards to the hydrodynamic model. Therefore, the good agreement between chlorophyll-a concentration and the model

thermocline further validates the skill of the model in representing the variability of the Cariaco basin surface layers.

The relation between the thermocline depth and the easterly winds speed has also been assessed. Inside the Cariaco basin, the thermocline responds to higher winds by rising, therefore causing an upwelling along the coast. Outside the Cariaco basin, higher winds increase the mixing of the ocean surface layers, and a deepening of the thermocline is thus observed. At short-time scales, it has been observed that the thermocline reacts mostly to the dynamics of the Caribbean Sea, mainly the presence of cyclonic and anticyclonic eddies in the Caribbean Current. The influence of the Caribbean cyclonic and anticyclonic eddies in the rising and lowering of isopycnals at the Tortuga channel has also been described by Astor et al. (2003) and Alvera-Azcárate et al. (2009a).

The analysis of the thermocline depth, wind speed and chlorophyll-a concentration has revealed that the Cariaco basin waters and the open Caribbean Sea waters are characterised by two distinct regimes. Open ocean waters thermocline depth deepens because of the increased mixing induced by winds. Inside the basin, however, increasing winds induce an upwelling response in the water column, and therefore the thermocline rises, bringing nutrient-rich waters to the surface and therefore increasing the amount of chlorophyll-a.

Finally, two ventilation events were observed in the Cariaco basin in 2004, detected as a deepening of the oxic–anoxic interface within the basin caused by the entrance of Caribbean subsurface water into the basin. A good correspondence between these events and the rising of the model thermocline along the Tortuga channel has been found. It has been verified that anticyclonic eddies were present in the Caribbean Sea during the two ventilation events, which could have therefore played a role in the ventilation of the basin. However, anticyclonic eddies were also present at other moments of the year. Therefore, although the ventilation of the Cariaco basin appears to occur when an anticyclonic eddy approaches the basin, not all anticyclonic eddies traveling along the Caribbean Current results in the ventilation of the basin. Other factors can be important for these events, such as the strength or positioning of the eddies, as well as the particular state of the Cariaco basin when the eddies approach the basin, the dominant currents or the vertical structure of the water column.

The good agreement between the model thermocline depth and independent variables such as the surface chlorophyll-a concentration and the oxic–anoxic interface derived from oxygen profiles shows the capability of the model to represent the thermocline position and its variability. In addition, it serves as an indirect validation of the fitting method used to characterise the depth of the thermocline.

Further research, based on the continuation of the observational work under way within the CARIACO program and on modelling studies such as the one presented in this work, are necessary to understand the influence of the open ocean in the Cariaco basin.

Acknowledgements

The authors wish to acknowledge the personnel of Fundacion La Salle, Estacion de Investigaciones Marinas (FLASA/EDIMAR), Venezuela; the crew of the R/V Hermano Ginés; and especially, Yrene Astor for the CTD and oxygen data. These data were taken as part of the CARIACO Time Series program, funded by the National Science Foundation (grant OCE-0326268). This work was also supported by the ONR grant N00014-05-1-0483. SeaWiFS chlorophyll-a concentration satellite data were provided by the NASA Goddard Space Flight Center and obtained through the website http://oceancolor.gsfc.nasa.gov/. The AVHRR Oceans Pathfinder SST data were obtained through the online PO.DAAC Ocean ESIP Tool (POET) at the Physical Oceanography Distributed Active Archive Center (PO.DAAC), NASA Jet Propulsion Laboratory, Pasadena, CA. http://podaac.jpl.nasa.gov/poet. The National Fund for Scientific Research, Belgium, is acknowledged for funding the post-doctoral positions of A. Alvera-Azcárate and A. Barth. We wish to acknowledge two anonymous reviewers for their useful comments.

References

Alexander, M., Scott, J., Deser, C., 2000. Processes that influence sea surface temperature and ocean mixed layer depth variability in a coupled model. Journal of Geophysical Research 105 (C7), 16823–16842.

Alvera-Azcárate, A., Barth, A., Beckers, J.-M., Weisberg, R.H., 2007. Multivariate reconstruction of missing data in sea surface temperature, chlorophyll and wind satellite fields. Journal of Geophysical Research 112, C03008 . doi:10.1029/2006JC003660.

Alvera-Azcárate, A., Barth, A., Rixen, M., Beckers, J.-M., 2005. Reconstruction of incomplete oceanographic data sets using empirical orthogonal functions. Application to the adriatic sea surface temperature. Ocean Modelling 9, 325–346 . doi:10.1016/j.ocemod.2004.08.001.

Alvera-Azcárate, A., Barth, A., Weisberg, R.H., 2009a. A nested model of the Cariaco Basin (Venezuela): description of the basin interior hydrography and interactions with the open ocean. Ocean Dynamics 59, 97–120 . doi:10.1007/s10236-008-0169-y.

Alvera-Azcárate, A., Barth, A., Weisberg, R.H., 2009b. The surface circulation of the Caribbean Sea and the Gulf of Mexico as inferred from satellite altimetry. Journal of Physical Oceanography 39, 640–657.

Astor, Y.M., Müller-karger, F., Scranton, M.I., 2003. Seasonal and interannual variation in the hydrography of the Cariaco Basin: implications for basin ventilation. Continental Shelf Research 23, 125–144.

Barth, A., Alvera-Azcárate, A., Weisberg, R.H., 2008a. A nested model study of the loop current generated variability and its impact on the West Florida Shelf. Journal of Geophysical Research 113, C05009. doi:10.1029/2007JC004492.

Barth, A., Alvera-Azcárate, A., Weisberg, R.H., 2008b. Benefit of nesting a regional model into a large-scale ocean model instead of climatology. Application to the West Florida Shelf. Continental Shelf Research 28, 561–573. doi:10.1016/j.csr.2007.11.004.

Beckers, J.-M., Rixen, M., 2003. EOF calculations and data filling from incomplete oceanographic data sets. Journal of Atmospheric and Oceanic Technology 20 (12), 1839–1856.

Chassignet, E.P., Hurlburt, H.E., Smedstad, O.M., Halliwell, G.R., Hogan, P.J., Wallcraft, A.J., Baraille, R., Bleck, R., 2007. The HYCOM (hybrid coordinate ocean model) data assimilative system. Journal of Marine Systems 65 (1–4), 60–83.

Coleman, T.F., Li, Y., 1996. An interior trust region approach for nonlinear minimization subject to bounds. SIAM Journal on Optimization 6 (2), 418–445.

Di Lorenzo, E., Miller, A.J., Schneider, N., McWilliams, J.C., 2005. The warming of the California current system: dynamics and ecosystem implications. Journal of Physical Oceanography, 336–362.

Ducet, N., Le Traon, P.Y., Reverdin, G., 2000. Global high resolution mapping of ocean circulation from the combination of TOPEX/Poseidon and ERS-1/2. Journal of Geophysical Research 105 (C8), 19477–19498.

Fairall, C.W., Bradley, E.F., Rogers, J.B., Edson, J.B., Young, G.S., 1996. Bulk parameterization of air–sea fluxes for tropical ocean-global atmosphere coupled-ocean atmosphere response experiment. Journal of Geophysical Research 101 (C2), 3747–3764.

Gill, A.E., 1982. Atmosphere-Ocean Dynamics. Academic Press.

Kalnay, E., Kanamitsu, M., Kistler, R., Collins, W., Deaven, D., Gandin, L., Iredell, M., Saha, S., White, G., Woollen, J., Zhu, Y., Leetmaa, A., Reynolds, R., Chelliah, M., Ebisuzaki, W., Higgins, W., Janowiak, J., Mo, K., Ropelewski, C., Wang, J., Jenne, R., Joseph, D., 1996. The NCEP/NCAR 40-year reanalysis project. Bulletin of the American Meteorological Society 77 (3), 437–471.

Kara, A.B., Rochford, P.A., Hurlburt, H., 2000. An optimal definition for ocean mixed layer depth. Journal of Geophysical Research 105 (C7), 16803–16821.

Kim, H.-J., Miller, A., 2007. Did the thermocline deepen in the California current after the 1976/77 climate regime shift? Journal of Physical Oceanography 37 (6), 1733.

Le Traon, P.Y., Nadal, F., Ducet, N., 1998. An improved mapping method of multisatellite altimeter data. Journal of Atmospheric and Oceanic Technology 15 (2), 522–534.

Mellor, G., Yamada, T., 1982. Development of a turbulence closure model for geophysical fluid problems. Reviews of Geophysics 20, 851–875.

Muller-Karger, F., Varela, R., Thunell, R., Scranton, M., Bohrer, R.G.T., Capelo, J., Astor, Y., Tappa, E., Ho, T.-Y., Walsh, J., 2001. Annual cycle of primary production in the Cariaco Basin: response to upwelling and implications for vertical export. Journal of Geophysical Research 106 (C3), 4527–4542.

Muller-Karger, F.E., McClain, C.R., Fisher, T.R., Esaias, W.E., Varela, R., 1989. Pigment distribution in the Caribbean Sea: observations from space. Progress in Oceanography 23, 23–64.

Muller-Karger, F.E., Varela, R., Thunell, R.C., Scranton, M.I., Taylor, G.T., Astor, Y., Benitez-Nelson, C.R., Lorenzoni, L., Tappa, E., Goñi, M.A., Rueda, D., Hu, C., 2010. The CARIACO oceanographic time series. In: Dummy, D. (Ed.), Carbon and Nutrient Fluxes in Continental Margins: A Global Synthesis. JGOFS Continental Margins Task Team (CMTT). Springer-Verlag, pp. 454–464.

Palacios, D.M., Bograd, S.J., Mendelssohn, R., Schwing, F.B., 2004. Long-term and seasonal trends in stratification in the California current, 1950–1993. Journal of Geophysical Research 109 (C10016), 1. doi:10.1029/2004JC002380.

Scranton, M.I., Astor, Y.M., Bohrer, R., Ho, T.-Y., Müller-karger, F., 2001. Controls on temporal variability of the geochemistry of the deep Cariaco Basin. Deep-Sea Research, I 48, 1605–1625.

Shchepetkin, A., McWilliams, J., 2005. The regional oceanic modeling system: a split-explicit, free-surface, topography-following-coordinate ocean model. Ocean Modelling 9, 347–404.

Soetaert, K., Hermana, P.M.J., Middelburg, J.J., Heip, C., Smith, C.L., Tett, P., Wild-Allen, K., 2001. Numerical modelling ofthe shelfbreak ecosystem: reproducing benthic and pelagic measurements. Deep-Sea Research 48, 3141–3177.

Steyn, D.G., Baldi, M., Hoff, R.M., 1999. The detection of mixed layer depth and entrainment zone thickness from lidar backscatter profiles. Journal of Atmospheric and Oceanic Technology 16 (7), 953–959.

Thomson, R., Fine, I.V., 2003. Estimating mixed layer depth from oceanic profile data. Journal of Atmospheric and Oceanic Technology 20 (2), 319–329.

Valiela, I., 1995. Marine Ecological Processes. Springer, 686pp.